N88-21525

A CONSTITUTIVE MODEL FOR AN OVERLAY COATING

D.M. Nissley, G.A. Swanson
Pratt & Whitney
East Hartford, Connecticut 06108

Coatings are frequently applied to gas turbine blades and vanes to provide protection against oxidation and corrosion. One class of coatings, known as overlay, usually has a nickel base with various protective elements added. Since no strengthening elements are included, it has a very low strength and becomes highly inelastic in real turbine airfoil applications. By contrast, turbine blades and vanes are cast from highly strengthened superalloys, which experience very little plasticity even though the thermomechanical loadings are severe. Strains generated in the superalloy airfoils during engine operation are imposed on the much thinner and weaker coating, subjecting it to severe cyclic damage, which leads to cracking of the coating. These cracks, in turn, are fatigue initiation sights for the airfoil. Hence, the inelastic behavior of the overlay coating plays an integral role in controlling the thermomechanical fatigue life of an advanced turbine blade or vane. This paper reports the results of an experimental and analytical study to develop a constitutive model for an overlay coating. Specimens were machined from a hot isostatically pressed (HIP) billet of PWA 286 (NiCoCrAlY + Hf + Si). The tests consisted of isothermal stress relaxation cycles with monotonically increasing maximum strain and were conducted at various temperatures. The results were used to calculate the constants for various constitutive models, including the classical, the Walker isotropic, a simplified Walker, and the Stowell models. A computerized regression analysis was used to calculate model constants from the data. The best fit (lowest standard deviation) was obtained for the Walker model, with the simplified Walker and classical models close behind. The Stowell model gave the poorest correlation.

Nomenclature

σ = stress (psi)

ε_t = total strain (in/in)

ε_e = elastic strain (in/in)

ε_{in} = $\varepsilon_p + \varepsilon_c$ = inelastic strain (in/in)

$\dot{\varepsilon}_{in}$ = inelastic strain rate (sec^{-1})

ε_p = plastic strain (in/in)

ε_c = creep strain (in/in)

$\varepsilon_{in\ eff}$ = effective inelastic strain (in/in)

$\dot{\varepsilon}_{in\ eff}$ = effective inelastic strain rate (sec^{-1})

E = elastic modulus (psi)

t = time (sec)

T = absolute temperature (°R)

R = universal gas constant ($1545\ \frac{\text{ft-lbf}}{\text{lb}_m\text{-mole-°R}}$)

ΔH = apparent activation energy ($\frac{\text{ft-lbf}}{\text{lb}_m\text{-mole}}$)

Ω = instantaneous back stress (kinematic hardening parameter) (psi)

Ω_2 = component of instantaneous back stress (psi)

K = instantaneous drag stress (isotropic hardening parameter) (psi)

Temperature dependent material constants (in consistent units):

$A_1, A_2, A_3, A_4, n, n_1, n_7, n_9, n_{10}, n_{11}, m_0, K_1, K_2, s, \sigma_0$

Introduction

One of the major goals of the NASA Hot Section Technology (HOST) program, which has sponsored this work, is the investigation and development of improved durability models for gas turbine hot section alloys. This broad activity addresses the durability issue considering both crack initiation and crack propagation of traditional isotropic (polycrystalline) and anisotropic (single crystal and directionally solidified) materials.

In application, many hot section components are coated to prevent oxidation and corrosion damage (e.g., combustors and turbine vanes and blades). Traditionally, coated thermomechanical fatigue life prediction methods applied to those components simply correlated coated specimen lives without regard to coating/substrate interactions. Although the significant effect of coatings on component thermomechanical fatigue life has been established (References 1-9), little experimental or analytical work has been conducted to evaluate the coating constitutive behavior necessary to provide input to a coating cracking life prediction model.

In this paper, the application of four constitutive models: (1) Classical, (2) Walker isotropic, (3) simplified form of Walker isotropic, and (4) the Stowell equation to NiCoCrAlY overlay coating behavior is presented. Initially, the models are applied to a baseline data set which represents typical low and high temperature tests conducted to obtain model constants. Next, each model is used to predict a thermomechanical cycle verification data set. To facilitate model-to-model comparisons, an identical baseline data set and automated material constant regression technique was used for each model. Standard deviation between the observed and calculated coating stress was used as the quantitative comparison criteria for the baseline data. Finally, a simple two-bar mechanism analysis of a coating/substrate composite structure, exposed to an out-of-phase thermomechanical cycle, is presented to demonstrate the vast dissimilarity between coating and substrate behavior.

Material and Test Specimen Descriptions

NiCoCrAlY + Si + Hf (PWA 286) is a typical vacuum plasma sprayed overlay type coating used to provide oxidation protection of gas turbine airfoil superalloys. Overlay coatings are easily distinguishable from diffusion type coatings in that virtually no interfacial diffusion zone occurs as a result of the application process. Due to that fact and also the small grained structure of overlay coatings in general, PWA 286 is considered isotropic in the plane of the airfoil surface. As such, bulk specimens were considered useful in determining overlay coating constitutive behavior.

The PWA 286 tested in this research effort was obtained in powder form, hot isostatically pressed (HIP) into an ingot, and then heat treated per normal engine hardware specifications. Constitutive specimens for both isothermal and thermomechanical experiments were then machined from the ingot into the geometry presented in Figure 1. In general, the airfoil applied coating contains some porosity near the coating/substrate interface region which was not observed in the specimen due to the HIP fabrication process.

Test Facility

The test facility used for the isothermal baseline tests included a servo-controlled, closed loop screw driven testing machine with set point controllers, an electrical resistance clamshell furnace, and a thermocouple for temperature monitoring. Axial deflection measurement was accomplished with a capacitance type extensometer. The extensometer specimen contact arms were placed into small dimples located at the gage section extremities.

The test facility used for the thermomechanical verification test included a servo-controlled, closed loop hydraulic testing machine with MTS controllers, a 7.5 kW - 10 kHz TOCCO induction heater, and an Ircon infrared radiation pyrometer for temperature measurement. Axial deflection measurement was accomplished with an MTS extensometer. The extensometer quartz rods, which define a one-inch gage section, are spring loaded against the specimen and did not show any signs of slippage during testing.

Baseline Data

The baseline data consists of isothermal stress relaxation experiments of the sort shown schematically in Figure 2. Although the baseline tests were conducted at several elevated temperatures spanning the operating range of 1000-2000°F, the present discussion is limited to the 1000°F and 1800°F data which is representative of low and high temperature behavior. The data from these two experiments are presented in Figure 3. Similar information at other temperatures is available in Reference 1.

Candidate Constitutive Models

For the sake of simplicity, only the one-dimensional forms of the models that were used to correlate the uniaxial data are discussed. Expanding the models into three-dimensional forms required by nonlinear finite element computer codes was considered unnecessary until such time that the most promising candidate model is chosen for continued development.

o Classical

The classical approach (e.g., Reference 10) was one of the first attempts at developing a nonlinear model which recognized the observed dissimilarity between monotonic tensile and creep inelastic material response. Time independent inelasticity (plasticity) and time dependent inelasticity (creep) are considered as uncoupled components of the total inelastic strain.

$$\varepsilon_{in} = \varepsilon_p + \varepsilon_c \tag{1}$$

Thus, the total strain function, neglecting thermal strain, is written:

$$\varepsilon_t = \varepsilon_e + \varepsilon_p + \varepsilon_c \tag{2}$$

or

$$\varepsilon_t = \sigma/E + f(\sigma) + g(\sigma,t) \tag{3}$$

Both plastic and creep strain functions $f(\sigma)$, $g(\sigma,t)$ are chosen to provide adequate duplication of the material behavior. From tests of PWA 286, it was determined that both functions could be described by simple power law relationships:

$$df = \frac{A_2}{A_1}\left(\frac{\sigma}{A_1}\right)^{A_2-1} d\sigma \tag{4}$$

$$dg = \left(\frac{\sigma}{A_3}\right)^{A_4} dt \tag{5}$$

o Walker

The Walker model (Reference 11) is among a new generation of constitutive models based on a unified viscoplastic approach which considers all nonlinear behavior as time dependent inelasticity. No distinction is made between plastic and creep inelastic action as in the Classical model. Walker, from his earlier work on Hastelloy X, chose to express inelastic behavior by a power law relationship which can be written as:

$$\dot{\varepsilon}_{in} = \left(\frac{\sigma-\Omega}{K}\right)^n \tag{6}$$

where n is a constant and Ω, back stress, and K, drag stress, are strain history dependent internal state variables which describe kinematic and isotropic cyclic hardening, respectively.

The back stress term is a quantity which physically corresponds to the asymptotic stress state under relaxation conditions. Qualitatively, the evolutionary expression for back stress is a sum of opposing hardening and thermal and dynamic recovery components which can be characterized as:

$$\dot{\Omega} = f\,(\dot{\varepsilon}_{in},\ \varepsilon_{in},\ T,\ t) - g\,(\dot{\varepsilon}_{in},\ \Omega,\ T,\ t) \tag{7}$$

Drag stress is a quantity which represents a resistance to inelastic flow, and is considered a function of the effective strain, $\varepsilon_{in\ eff}$.

$$K = K_1 - K_2 \exp\,(-n_7\ \varepsilon_{in\ eff}) \tag{8}$$

where: K_1 = fully hardened/softened drag stress

$K_1 - K_2$ = initial drag stress.

Thus, the drag stress function is a monotonically increasing relationship describing isotropic hardening ($K_2>0$) or softening ($K_2<0$). The Walker model form used for this investigation is given below:

$$\dot{\varepsilon}_t = \dot{\varepsilon}_e + \dot{\varepsilon}_{in} \tag{9a}$$

$$\dot{\varepsilon}_{in} = \left(\frac{\sigma-\Omega}{K}\right)^n \tag{9b}$$

$$K = K_1 - K_2 \exp\,(-n_7\ \varepsilon_{in\ eff}) \tag{9c}$$

$$\Omega = n_1\ \varepsilon_{in} + \Omega_2 \tag{9d}$$

$$\dot{\Omega}_2 = n_{11}\ \dot{\varepsilon}_{in} - \Omega_2\ (\dot{G}_2 - \frac{1}{n_{11}} \frac{\partial n_{11}}{\partial T}\ \frac{dT}{dt}\ ) \tag{9e}$$

$$\dot{G}_2 = n_9\ \dot{\varepsilon}_{in\ eff} + n_{10}\,\Omega_2^{(m_o-1)} \tag{9f}$$

$$\dot{\varepsilon}_{in\ eff} = |\dot{\varepsilon}_{in}| \tag{9g}$$

References 11 and 12 provide a detailed discussion of Walker's and other unified approaches.

o Simplified Walker

This model is identical to the Walker model except that all back stress terms were eliminated.

$$\dot{\varepsilon}_{in} = (\sigma/K)^n \tag{10}$$

the expression for $\dot{\varepsilon}_{in}$ is equivalent to the Classical model power law creep equation; however, in this case, the drag stress term, K, is not a constant, but an evolutionary variable. From a simplicity standpoint, this model is very attractive.

o Stowell

The Stowell model (References 13 through 15) is another form of a unified viscoplastic approach initially developed to simulate heating rate effects on yielding of metals. It considers inelastic action based on an apparent activation energy level and uses a hyperbolic sine stress function.

$$\dot{\varepsilon}_{in} = 2s\ T \exp\left(\frac{-\Delta H}{RT}\right) \sinh\left(\frac{\sigma}{\sigma_o}\right) \tag{11}$$

Verification Data

Qualitative evaluation of the predictive capabilities of the candidate constitutive models was accomplished by application to verification data consisting of an out-of-phase thermomechanical waveform. Thermomechanical cycles include complex material behavior such as stress relaxation and plasticity which is useful for exercising the models. The out-of-phase cyclic condition is of particular interest in that such conditions are typical of gas turbine airfoil external surfaces where many thermomechanical fatigue cracks originate in the coating.

Correlation of Baseline Data

Baseline data correlation by each candidate constitutive model is presented in Figures 4 and 5, and a summary of the corresponding standard deviations is given in Table I. The material constants for each model obtained from the baseline tests are presented in Table II.

As expected, the Classical model regression indicated that plasticity dominates the inelastic response at low temperature while creep dominates at high temperature. The Walker and Simplified Walker models correlate the data similarly. It seems that the added complexity of incorporating back stress is unnecessary for modeling this isothermal data set. The Stowell model correlated the baseline information the poorest.

Based on standard deviation and the given baseline data set, the candidate constitutive models can be listed in order of correlation capability as follows: (1) Walker, (2) Simplified Walker, (3) Classical, and (4) Stowell.

Prediction of Thermomechanical Verification Data

Experimental and predicted thermomechanical fatigue (TMF) waveforms are presented in Figure 6.

The high temperature response of the TMF cycle was fairly well predicted by all the models, but none were able to predict the extent of the low temperature tensile inelasticity. In fact, only the Walker and Classical models managed to predict any low temperature yielding. The Simplified Walker and Stowell models predicted thermoelastic tensile responses.

The ability of the Walker model to predict the observed tensile yielding trend can be explained as follows: during the compression/heating portion of the cycle (points A to B), the material relaxes, creating a compressive back stress. Then, during the tensile/cooling portion of the cycle (points B to C), the back stress moves deeper into compression due to temperature rate effects. Thus, the "effective" stress (σ-Ω), at which yielding initiates, occurs at a lower applied tensile stress.

The ability of the Classical model to predict some low temperature yielding reflects the fact that this model did not reproduce the observed low temperature yielding trend. Had the Classical model correlated the 1000°F behavior better, it is felt that the low temperature tensile portion of the TMF prediction would have been more like the Simplified Walker and Stowell models...thermoelastic.

Simulation of Coated Superalloy Constitutive Behavior

A simple one dimensional two-bar mechanism simulation of coating and substrate constitutive behavior was performed to help visualize the coating response to TMF cycling as would occur on an airfoil. A schematic of the two-bar mechanism and the predicted results are presented in Figure 7.

A thermo-elastic creep model was used for the PWA 1480 <001> and the Walker model was used for the PWA 286. Note that the mechanical strain range of the PWA 286 is 0.25 percent higher than the PWA 1480 substrate. This is due to the thermal growth and strength characteristics of both materials. Upon load reversal, high stress and plasticity are generated in the coating as the structure is cooled.

Summary and Conclusions

1. Four candidate coating constitutive models were evaluated based on the ability to correlate a baseline data set consisting of isothermal stress relaxation experiments. The four models presented can be ranked as follows: (1) Walker, (2) Simplified Walker, (3) Classical, and (4) Stowell based on the standard deviation of the correlation.

2. An out-of-phase thermomechanical cycle was used to evaluate the four candidate models. Although none of the models accurately predicted the TMF cycle, a back stress formulation such as is incorporated in the Walker model is considered necessary to duplicate the observed material behavior.

3. A one-dimensional two bar mechanism was utilized to calculate PWA 286 coating behavior on a PWA 1480 <001> substrate during out-of-phase thermomechanical cycling. The coating was predicted to have significantly larger mechanical strain range and reverse inelasticity than the PWA 1480 substrate.

Acknowledgements

The experimental testing and analytical work were conducted by Pratt & Whitney, United Technologies Corporation, East Hartford, Connecticut under sponsership of the NASA Lewis Research Center, Contract NAS3-23939.

References

1. G. A. Swanson, I. Linask, D. M. Nissley, P. P. Norris, T. G. Meyer, K. P. Walker, "Life Prediction and Constitutive Models for Engine Hot Section Anisotropic Materials Program; First Annual Report," NASA CR-174952, February, 1986.

2. K. R. Bain, "The Effect of Coatings on the Thermomechanical Fatigue Life of a Single Crystal Turbine Blade Material," 21st Joint Propulsion Conference, AIAA-85-1366, July, 1985.

3. D. P. DeLuca and B. A. Cowles, "Fatigue and Fracture of Advanced Blade Materials," Final Report to AFWAL, FR-18518, Pratt & Whitney, 1984.

4. R. H. Barkalow, "Effect of Cyclic Strain/Temperature Exposure on Fatigue Life of Coated Turbine Alloys," Interim Report to AFWAL/ML, FR-18605, Pratt & Whitney, September, 1984.

5. P. K. Wright, "TMF Failure Models in Single Crystal Rene' N4," NASA TMF Workshop, November 15-16, 1984.

6. T. E. Strangman, "Thermal Fatigue of Oxidation Resistant Overlay Coatings," Ph.D. Thesis, University of Connecticut, 1978.

7. I. Linask and J. Dierberger, "A Fracture Mechanics Approach to Turbine Airfoil Design," ASME Gas Turbine Conference and Products Show, March 2-6, 1975.

8. M. Gell, G. R. Leverant and C. H. Wells, "The Fatigue Strength of Nickel-Base Superalloys," Achievement of High Fatigue Resistance in Metals and Alloys, STP 467, ASTM, 1970, pp. 113-153.

9. G. R. Leverant and M. Gell, "The Elevated Temperature Fatigue of a Nickel-Base Superalloy, Mar-M200," Trans. Metallurgical Society of AIME, Vol. 246, 1969, pp. 1167-1173.

10. H. Kraus, Creep Analysis, John Wiley & Sons, Inc., New York, Chapter 2, 1980.

11. K. P. Walker, "Research and Development Program for Nonlinear Structural Modeling with Advanced Time-Temperature Dependent Constitutive Relationships," NASA CR-165533, November, 1981.

12. U. S. Lindholm, et al, "Constitutive Modeling for Isotropic Materials (HOST)," NASA CR-174718, May, 1984.

13. E. Z. Stowell, et al, "Predicted Behavior of Rapidly Heated Metal in Compression," NASA TR R-59, 1960.

14. E. Z. Stowell, "The Properties of Metals Under Rapid Heating Conditions," J. Aeron Sci., pp. 922-923, December, 1957.

15. E. Z. Stowell, "A Phenomenological Relation Between Stress Strain Rate, and Temperature for Metals at Elevated Temperature," NASA TR-R1343, February, 1957.

Table I

Summary of Constitutive Model Regression Fit
Standard Deviation (1 std dev., in psi)

	1000°F	1400°F	1600°F	1800°F	2000°F
Walker	2000	1815	633	153	101
Simplified Walker	2041	1717	876	220	119
Classical	2255	1878	736	300	127
Stowell	6541	2091	1044	377	140

TABLE II

Summary of Constitutive Model Regressed Temperature Dependent Material Constants

	1000°F	1400°F	1600°F	1800°F	2000°F
E	.185E8	.1E8	.8E7	.3E7	.1E7
Walker					
n	26.85	3.318	2.240	2.036	1.649
n_1	1617.0	704.6	806.0	1316.0	1573.0
n_7	2369.0	1202.0	2653.0	1900.0	184.3
n_9	253.3	58.5	131.7	38.87	113.7
n_{10}	.2389E-4	.1469E-3	.5504E-3	.2184E-3	.1340E-3
n_{11}	.4955E7	.4006E6	.5625E6	.7500E5	.3312E5
m_0	1.2	1.2	1.2	1.2	1.2
K_1	.1736E6	.5845E6	.5410E6	.2053E6	.1435E6
K_2	.3315E5	.2048E6	.3624E6	-.1094E4	-.4711E5
Simplified Walker					
n	29.57	3.554	3.424	3.295	3.295
n_7	787.7	770.4	405.3	100.6	156.0
K_1	.1865E6	.5164E6	.1545E6	.5044E5	.1408E5
K_2	.4351E5	.2302E6	.4906E5	.2370E5	.5820E4
Classical					
A_1	.3054E6	.5153E6	.3325E6	.8385E5	.4753E5
A_2	7.579	2.711	2.026	2.261	2.183
A_3	.7778E6	.4885E6	.1928E6	.4861E5	.8368E4
A_4	7.325	3.627	3.207	3.214	3.909
Stowell					
s	.1156E-11	.7814E-10	.1529E-9	.1282E-8	.7478E-9
ΔH	.2198E7	.4471E6	.3640E6	.1668E7	.1121E7
σ_0	.1376E5	4971.	1682.	681.6	191.3

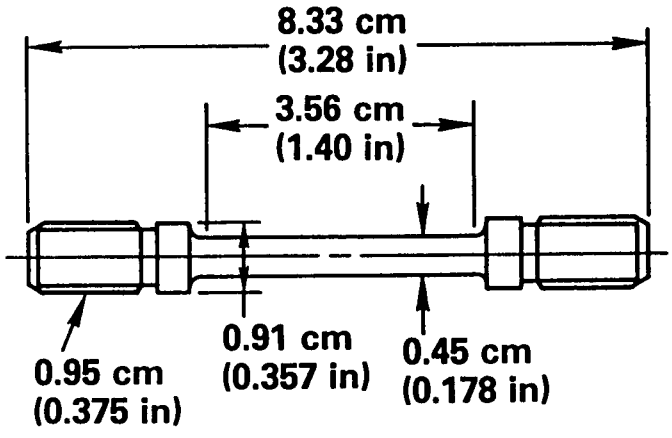

Figure 1 PWA 286 Stress Relaxation Specimen Design

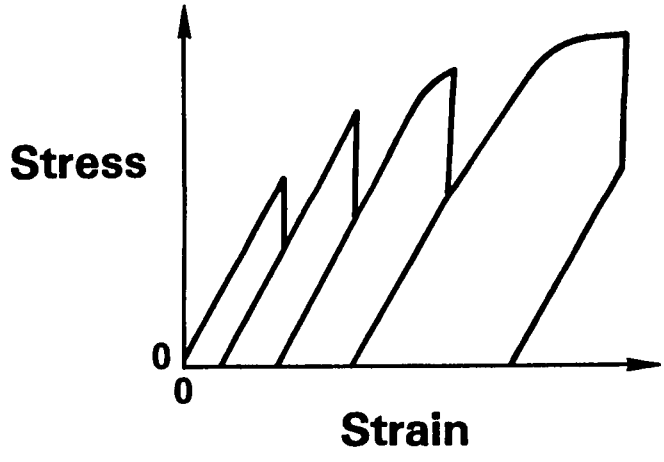

Figure 2 Typical Isothermal Stress Relaxation Experiment

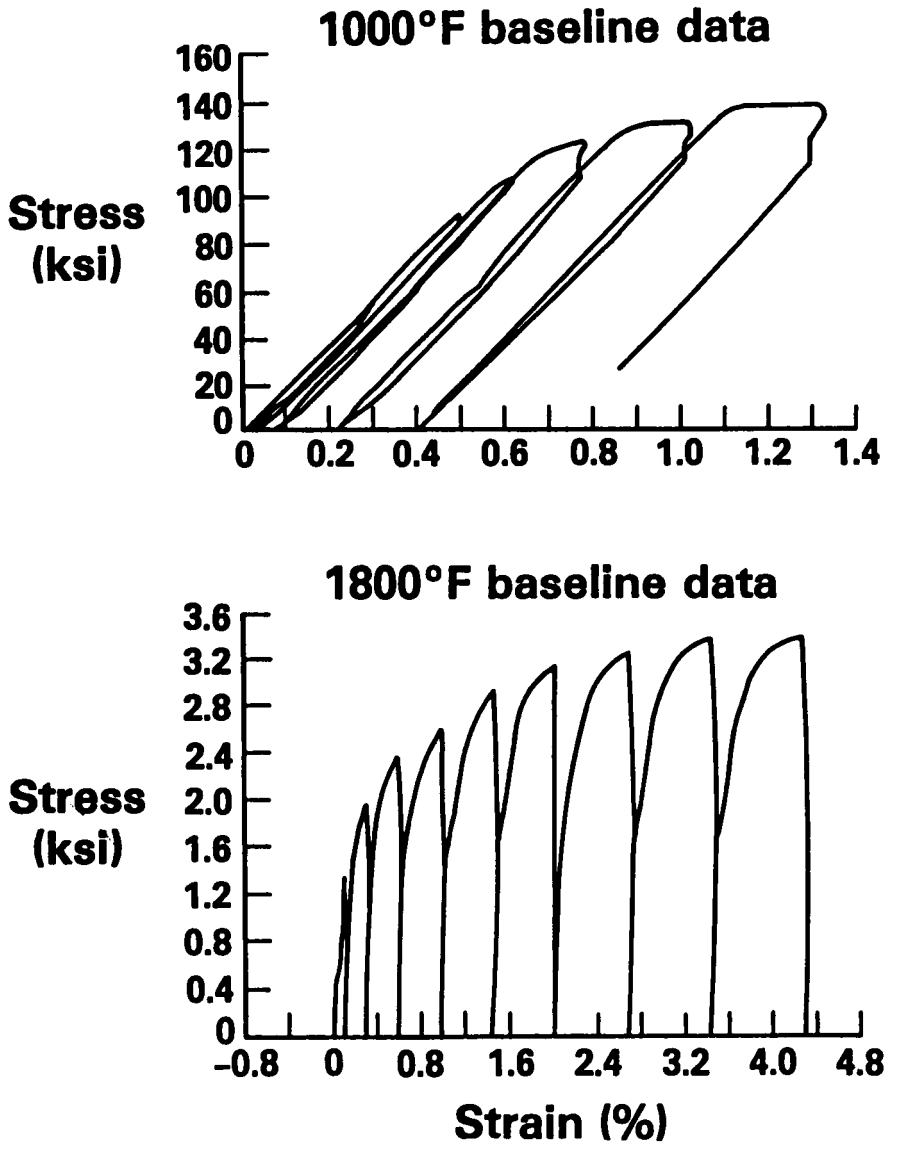

Figure 3 1000°F and 1800°F PWA 286 Baseline Stress Relaxation Data

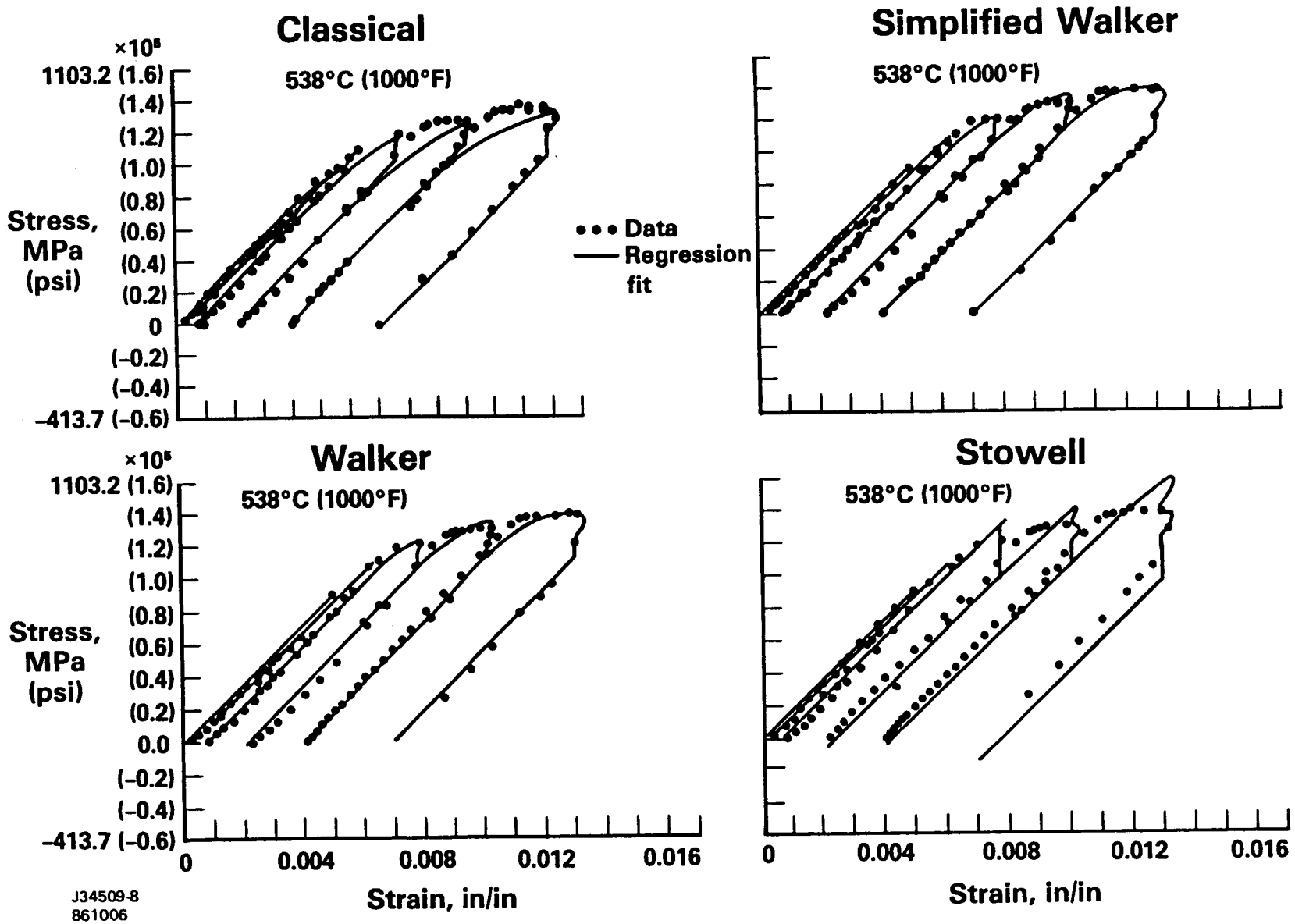

Figure 4 Low Temperature Regression Fit of PWA 286 Stress Relaxation Data

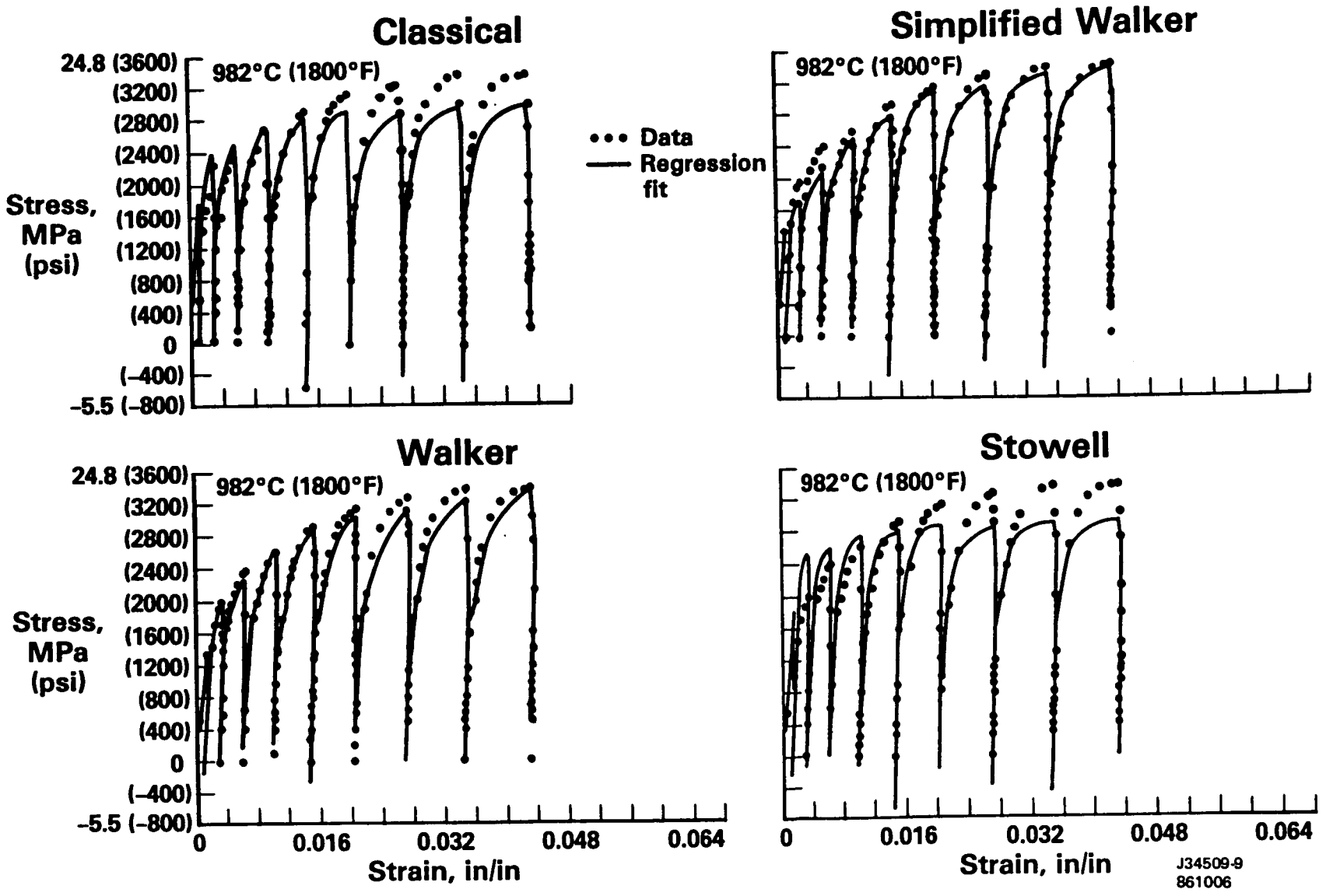

Figure 5 High Temperature Regression Fit of PWA 286 Stress Relaxation Data

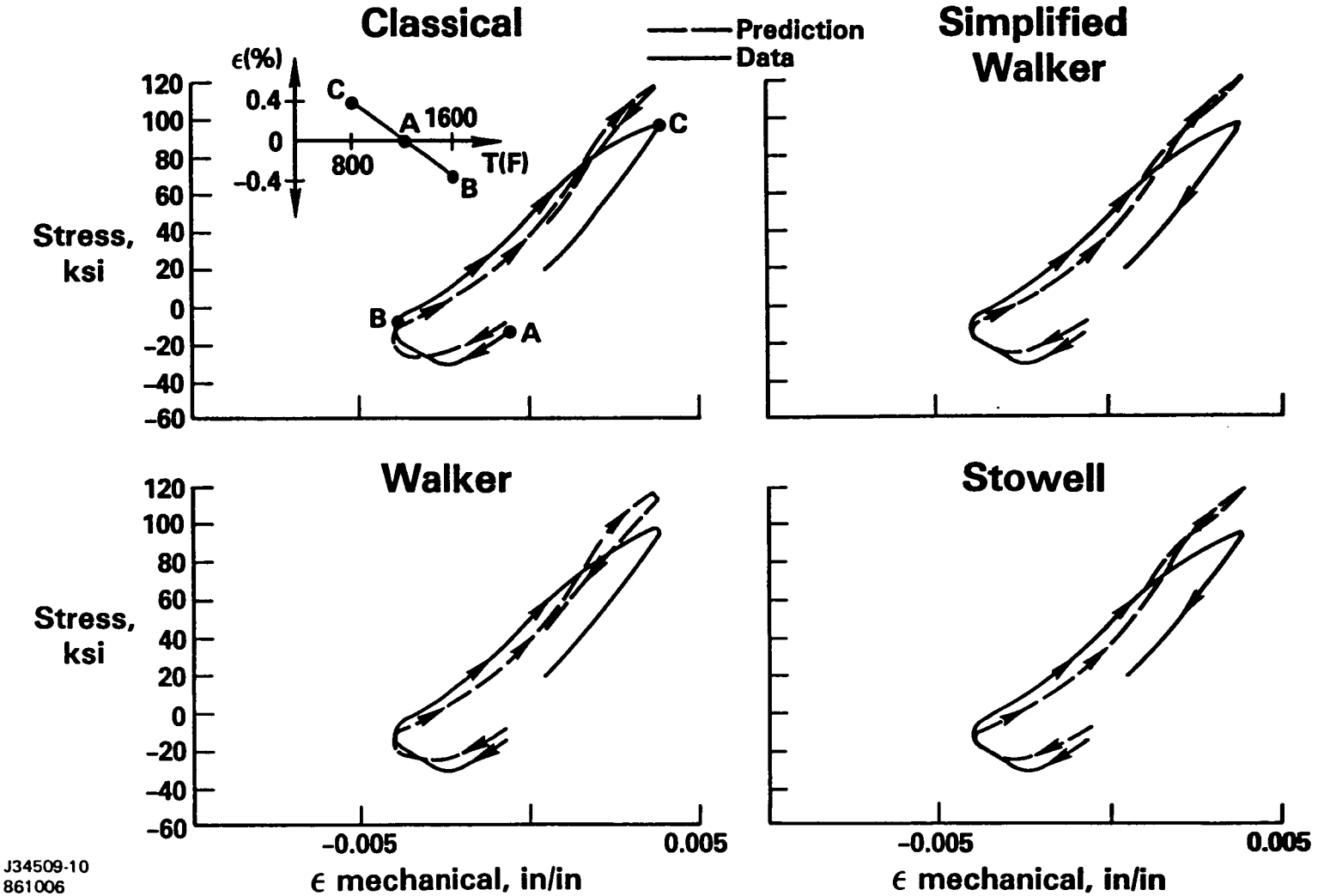

Figure 6 PWA 286 Thermo-Mechanical Test - 1st Cycle Prediction Vs. Test Data

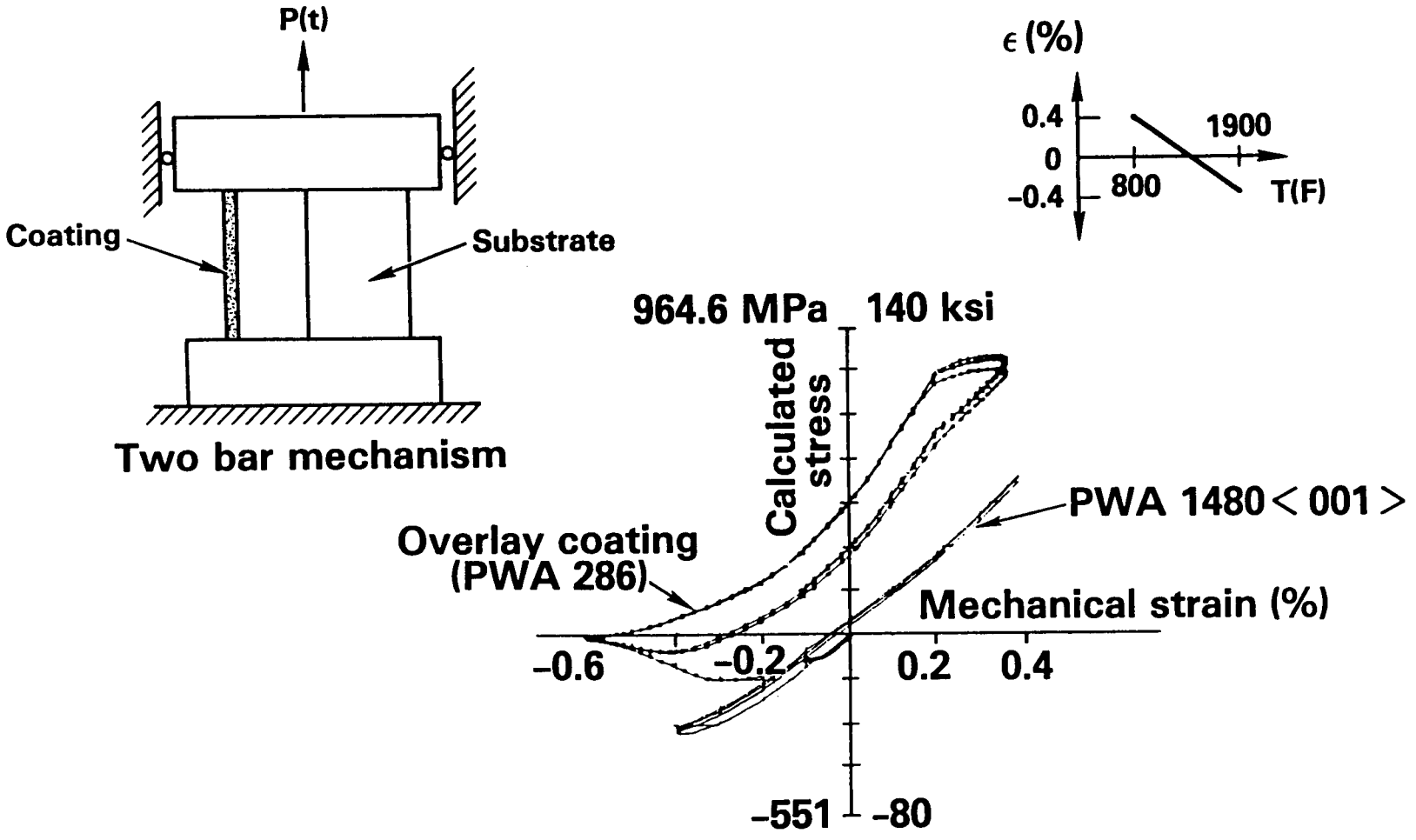

Figure 7 "Two-Bar" Mechanism and Predicted Coating/Substrate Hysteretic Response of a 427-1038°C (800-1900°F), ±0.4%, Out-of-Phase TMF Test